

Anomalous impurity effect in the heavy-fermion superconductor CeCu_2Si_2

Shan Zhao,¹ Weifu Liu,¹ Yi-feng Yang,^{2,3,4,*} Shiping Feng,⁵ and Bin Liu^{1,†}

¹*School of Physical Science and Engineering, Beijing Jiaotong University, Beijing 100044, China*

²*Beijing National Laboratory for Condensed Matter Physics,*

Institute of Physics, Chinese Academy of Science, Beijing 100190, China

³*School of Physical Sciences, University of Chinese Academy of Sciences, Beijing 100190, China*

⁴*Songshan Lake Materials Laboratory, Dongguan, Guangdong 523808, China*

⁵*Department of Physics, Beijing Normal University, Beijing 100875, China*

(Dated: August 16, 2024)

Recent observations of a contradictory impurity effect in the heavy-fermion superconductor CeCu_2Si_2 at ambient pressure have hindered the identification of its pairing symmetry. Here, we perform theoretical analyses with both intraband and interband impurity scatterings for the nodeless s^\pm -wave pairing, and report an anomalous nonmonotonic variation of its T_c suppression with the scattering strength. Our results reproduce the prominent reduction of T_c in good agreement with earlier experiments by atomic substitution and explains as well its robustness against electron irradiation. We ascribe the latter to the screening of the interband impurity potential in the strong scattering or unitary region. This resolves the seeming contradiction in different experimental probes and provides an important support to the nodeless s^\pm -wave scenario in CeCu_2Si_2 at ambient pressure. Our theory may be extended to other narrow-band systems such as twisted bilayer graphene and the recently discovered bilayer or trilayer nickelate superconductors, and provide a useful way to distinguish different pairing candidates thereof.

PACS numbers: 74.70.Tx, 74.20.Pq, 74.62.En

Identifying the pairing symmetry is a central yet extremely challenging issue for unconventional superconductors. One notable example is CeCu_2Si_2 ¹, which was discovered in 1979 as the first unconventional superconductor² and, for over 30 years, had been widely believed to be of d -wave pairing mediated by antiferromagnetic spin fluctuations^{3–7}. However, in 2014, more elaborate measurements of the specific heat and magnetization on high-quality samples down to 40 mK found surprising thermodynamic evidence for two nodeless gaps⁸ and thus questioned the hitherto prevailing d -wave scenario. This unexpected observation was subsequently confirmed by a series of refined experiments such as scanning tunneling microscopy (STM) down to 20 mK⁹, angle-dependent specific heat¹⁰, London penetration depth^{11–13}, thermal conductivity¹³, and angle-resolved photoemission spectroscopy (ARPES)¹⁴. A multiband picture was soon developed based on first-principles electronic band-structure calculations, claiming the importance of both electron and hole Fermi surfaces^{15,16}. Different pairing candidates have since been proposed including the sign reversal s^\pm wave due to a strong interband pairing interaction¹⁶, the sign preserving s^{++} wave¹³, and the “ $d+d$ ” mixed pairing motivated by the study of iron-pnictide superconductors^{11,17}. While all these proposals seem to fit well existing data of the specific heat^{8,10,13} and the London penetration depth^{11,13}, a direct experimental probe of the gap structures is lacking due to the limited energy resolution. As a result, the exact gap structures of superconducting CeCu_2Si_2 at ambient pressure still remain undecided.

It is therefore crucial to look for smoking gun evidence that may distinguish these different scenarios. Among all

possible probes, the impurity effect provides significant phase information on the pairing symmetry for both conventional and unconventional superconductors¹⁸. Actually, such experiments have been carried out on CeCu_2Si_2 shortly after its discovery and found that replacing Cu by merely about 1% Rh, Pd, or Mn¹⁹ can completely destroy the superconductivity. On the other hand, for substitution of the Ce sites, the suppression of T_c relies heavily on the dopant, with the critical concentration being 0.5% for Sc, 6% for Y, 10% for La, and 20% for Th^{19,20}. These earlier measurements on the pair breaking effects caused by impurities were believed to provide strong support for nodal d -wave pairing in CeCu_2Si_2 . But recent electron irradiation experiments reported surprising robustness of the superconductivity, thus hinting at a fully gapped s^{++} -wave pairing in contrast to similar measurements on cuprate and iron-pnictide superconductors with sign changing d - or s^\pm -wave gaps¹³. On the other hand, the s^\pm -wave pairing has been used to explain the neutron spin resonance mode^{6,21}, the absence of the Hebel-Slichter peak, and the $1/T_1 \propto T^3$ scaling of the spin-lattice relaxation rate^{22,23}.

In this paper, we investigate the impurity effect in superconductor CeCu_2Si_2 and show that the above controversy may be resolved based on the fully gapped sign reversal s^\pm -wave pairing state¹⁶. By using the Eliashberg gap functions and the T -matrix approach for a realistic two-band hybridization model, we present detailed theoretical studies on the suppression of T_c and the density of states (DOS) with the intraband impurity scattering strength u and the interband scattering strength v . We find a critical intraband scattering strength U_c controlled by the ratio $r = v/u$ and the DOS at the Fermi energy,

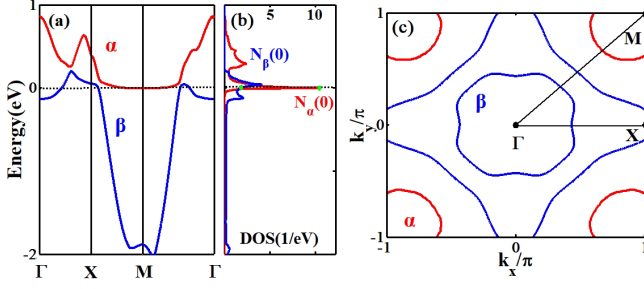


FIG. 1: (a) Electronic band structures of our effective two-band hybridization model from DFT+U for CeCu₂Si₂ at ambient pressure. (b) Density of states of the α and β bands in the normal state. $N_\alpha(0)$ and $N_\beta(0)$ refer to the DOS of α and β bands at the Fermi energy. (c) A typical mapping of the two-dimensional Fermi surfaces with the hole Fermi surface β and the heavy-electron Fermi surface α .

below which T_c is quickly suppressed with increasing impurity concentration, while beyond which the superconductivity gradually revives with increasing u and remains robust against impurities in the unitary limit. Such unexpected anomalous features reconcile the seeming discrepancy of the impurity effect induced by atomic substitution and electron irradiation, and hence provide important support for the fully gapped s^\pm pairing in the heavy-fermion superconductor CeCu₂Si₂ at ambient pressure.

Our effective two-band hybridization model^{24,25} is constructed based on density functional theory calculations (DFT+U), where only two hybridization bands cross the Fermi energy and dominate the low-energy physics of CeCu₂Si₂¹⁶. The electronic band structures are plotted in Fig. 1(a). A sharp peak is clearly seen in the DOS in Fig. 1(b), reflecting the extremely flat heavy electron band (α) of typical f character due to the many-body Kondo effect. At the Fermi energy, the DOS of the α band $N_\alpha(0)$ is about six times larger than that of the β band $N_\beta(0)$. For a strong interband pairing interaction¹⁶, this predicts a gap ratio $|\Delta^\beta/\Delta^\alpha| \approx [N_\alpha(0)/N_\beta(0)]^{1/2} \approx 2.4$, in good agreement with experimental estimates⁸⁻¹¹. A typical two-dimensional mapping in Fig. 1(c) shows multiple Fermi surfaces, which fit well the recent ARPES measurement¹⁴.

Without impurities, the linearized Eliashberg equation^{26,27} is written as

$$\Delta^i(i\omega_n) = -\pi T \sum_{j=\alpha,\beta} g_{ij} N_j \sum_m' \frac{\Delta^j(i\omega_m)}{|\omega_m|}, \quad (1)$$

where i, j denote the band indices, N_j refers to the DOS of band j at the Fermi energy, $\omega_{n/m}$ is the fermionic Matsubara frequency, and $\sum_m' \equiv \sum_m \theta(\omega_c - |\omega_m|)$, where ω_c is the cutoff. Clearly, the s^\pm -wave pairing is favored for a sufficiently large interband pairing interaction $g_{\alpha\beta} = g > 0$. To focus on the impurity effect, we have neglected for simplicity the mass enhancement and quasiparticle damping induced by an electron-electron interaction.

The effect of impurities can be well captured by the T -matrix approach as long as the concentration $n_{imp} \ll 1$. The normal and anomalous self-energies are then given respectively by

$$\begin{aligned} \Sigma_i^A(i\omega_n) &= n_{imp} \sum_{j=\alpha,\beta} T_{ij}(i\omega_n) f_j(i\omega_n) T_{ij}(-i\omega_n), \\ \Sigma_i^N(i\omega_n) &= n_{imp} T_{ii}(i\omega_n), \end{aligned} \quad (2)$$

where $f_j(i\omega_n) = \pi N_j \Delta^j(i\omega_n)/|\omega_n|$ represents the local anomalous Green's function, $T_{ij}(i\omega_n) = U_{ij} + \sum_{l=\alpha,\beta} U_{il} g_l(i\omega_n) T_{lj}(i\omega_n)$ is the T -matrix element for the nonmagnetic impurity scattering $U_{ij} = u\delta_{ij} + v(1 - \delta_{ij})$, and $g_l(i\omega_n) = -i\pi N_l \text{sgn}(\omega_n)$ is the local normal Green's function²⁷. Taking into account these impurity effect, the linearized gap equation becomes²⁷

$$Z_i(i\omega_n) \Delta^i(i\omega_n) = -\pi T \sum_{j=\alpha,\beta} g_{ij} N_j \sum_m' \frac{\Delta^j(i\omega_m)}{|\omega_m|} + \Sigma_i^A(i\omega_n), \quad (3)$$

with the renormalization function

$$Z_i(i\omega_n) = 1 - \frac{\Sigma_i^N(i\omega_n) - \Sigma_i^N(-i\omega_n)}{2i\omega_n}. \quad (4)$$

When only the interband pairing interaction is considered for the case of dominant s^\pm -wave pairing, we obtain the following equation for T_c

$$g^2 N_\alpha N_\beta (X - B)(X - C) - \frac{2g N_\alpha N_\beta}{N_\alpha + N_\beta} (C - B) = 1, \quad (5)$$

with

$$\begin{aligned} X &= \psi\left(\frac{\omega_c}{2\pi T_c} + 1\right), B = \psi\left(\frac{1}{2}\right), \\ C &= \psi\left(\frac{1}{2} + (N_\alpha + N_\beta) \frac{n_{imp} v^2}{2T_c D}\right), \end{aligned} \quad (6)$$

where $D = 1 + \pi^4 N_\alpha^2 N_\beta^2 (u^2 - v^2)^2 + \pi^2 u^2 (N_\alpha^2 + N_\beta^2) + 2\pi^2 v^2 N_\alpha N_\beta$ and $\psi(x)$ is the digamma function. For $n_{imp} \ll 1$, the above equation may be approximately solved and gives

$$\ln \frac{T_{c0}}{T_c} \approx \gamma \left[\psi\left(\frac{1}{2} + \frac{(N_\alpha + N_\beta) n_{imp} v^2}{2T_c D}\right) - \psi\left(\frac{1}{2}\right) \right], \quad (7)$$

where $T_{c0} \sim 0.6$ K is the superconducting transition temperature without impurities and $\gamma = 1/2 + \sqrt{N_\alpha N_\beta}/(N_\alpha + N_\beta)$. This expression is similar to previous results²⁷⁻²⁹ where T_c may be solved iteratively.

For comparison with experiments, we plot in Fig. 2(a) the variation of T_c/T_{c0} as a function of the impurity concentration n_{imp} for a typical ratio $v/u = 0.8$ in the Born or weak impurity scattering region (small u). As expected, T_c drops quickly with n_{imp} and the overall suppression is enhanced as the scattering potential u increases. This provides a potential explanation of earlier

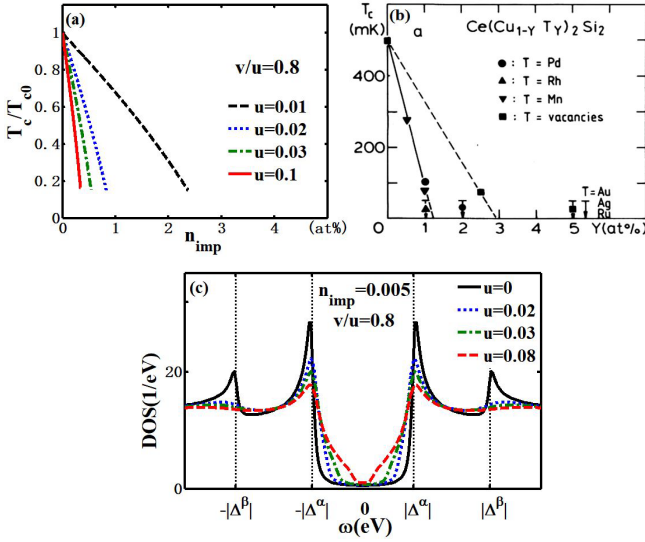


FIG. 2: (a) The calculated T_c/T_{c0} as a function of the impurity concentration n_{imp} for weak intraband impurity scattering u at a fixed ratio $v/u = 0.8$. (b) Variation of T_c of $CeCu_2Si_2$ with Cu substitutions in experiment, adapted from Ref.[19]. (c) Impurity-induced DOS for different values of u at $n_{imp} = 0.005$ and $v/u = 0.8$.

doping experiments reproduced in Fig. 2(b)¹⁹, where the superconductivity is destroyed in similar manners for 1% of Rh, Pd, or Mn replacement of Cu. Since Cu 3d orbital contributes little component of the Fermi surface evidenced by DFT+ U calculations¹⁴, its substitution is reasonably assumed to cause weak impurity scattering. Besides the suppression of T_c , the impurities also induce in-gap states. Figure 2(c) plots the DOS in the superconducting state derived from the imaginary part of the local Green's function for $n_{imp} = 0.005$. In contrast to two intragap resonance peaks for a single nonmagnetic impurity^{24,25,30}, an impurity band appears so that the original nearly U shaped DOS ($u = 0$) turns into a V shape at $u = 0.03$ and is almost filled in beyond $u = 0.08$. This DOS variation might explain the power-law behavior in $1/T_1$ in earlier NMR measurement and the larger full gap and smaller nodal gap in tunneling spectra⁹.

So far it looks normal, but surprises come from the substitution or removal of Ce sites. Since Ce 4f electrons dominate the superconductivity in $CeCu_2Si_2$, one may naively assume stronger impurity effect than those of Cu replacement. We have therefore performed further calculations for strong impurity scattering (large u). The resulting T_c/T_{c0} is plotted in Fig. 3(a) as a function of n_{imp} for the same ratio $v/u = 0.8$. Quite remarkably, instead of further suppressing T_c as in Fig. 2(a), the superconductivity seems to gradually revive with increasing u and is robust against the impurities in the unitary limit ($u = 10$). This suggests that very strong scattering potential (large u) has actually a weaker effect on T_c . Indeed, the critical concentrations for replacing Ce are 0.5% Sc, 6% Y, 10% La, or 20% Th in experiment

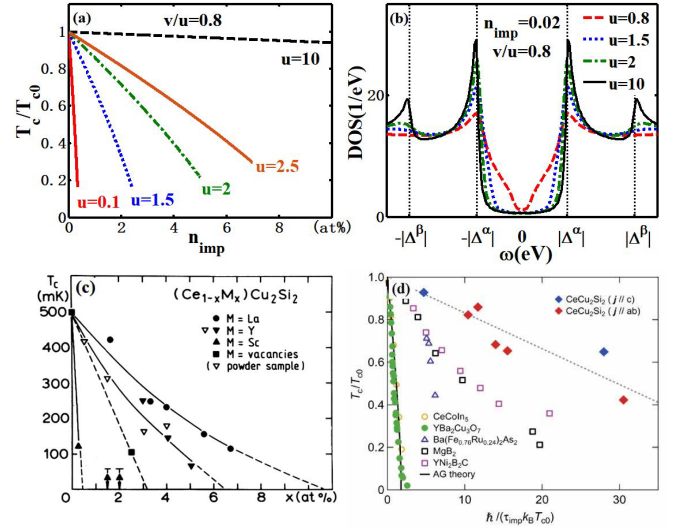


FIG. 3: (a) The calculated T_c/T_{c0} as a function of the impurity concentrations n_{imp} for strong intraband impurity scattering u at a fixed ratio $v/u = 0.8$. (b) Impurity-induced DOS for different values of u at $n_{imp} = 0.02$ and $v/u = 0.8$. (c) Variation of T_c of $CeCu_2Si_2$ with Ce substitutions adapted from Ref.[19]. (d) Comparison of electron irradiation measurements on T_c/T_{c0} in $CeCu_2Si_2$ and other superconductors adapted from Ref.[13].

as reproduced in Fig. 3(c)^{19,20}. In order to make a direct comparison with experimental data, in Fig. 3(a) we estimate the scattering potential $u = 0.1$ for Sc, $u = 2$ for Y, and $u = 2.5$ for La, respectively, since the scattering strength is believed to be in direct proportion to the ionic radius and the scattering cross section. In particular, removing some Ce ions by electron irradiation is expected to bring much stronger scattering than atomic substitution¹³. But as shown in Fig. 3(d) adapted from Ref.[13], its suppression on T_c is much slower than those in cuprate and iron-pnictide superconductors, but similar to conventional s -wave superconductors. Thus, the consistency between our theory and the experiments provides a potential explanation to the puzzling observation in the doping and electron irradiation experiments in $CeCu_2Si_2$, and consequently supports the nodeless s^{\pm} -wave pairing of its superconductivity. With increasing u , as shown in Fig. 3(b) for $n_{imp} = 0.02$, the DOS recovers from a V shape at $u = 0.8$ to a U shape at $u = 10$, reflecting the robustness of superconductivity even in the unitary limit. It should be noted that the exact strength of the scattering potential for each type of impurity is not known in $CeCu_2Si_2$. It will be important if future materials calculations or refined experiments could clarify this aspect in order to fully establish the above scenario.

The anomalous behavior of T_c suppression may be understood analytically from Eq. (7), where the difference of two digamma functions is fully determined by the magnitude of $(N_{\alpha} + N_{\beta})n_{imp}v^2/2T_cD$. This quantity increases linearly with n_{imp} , causing the mono-

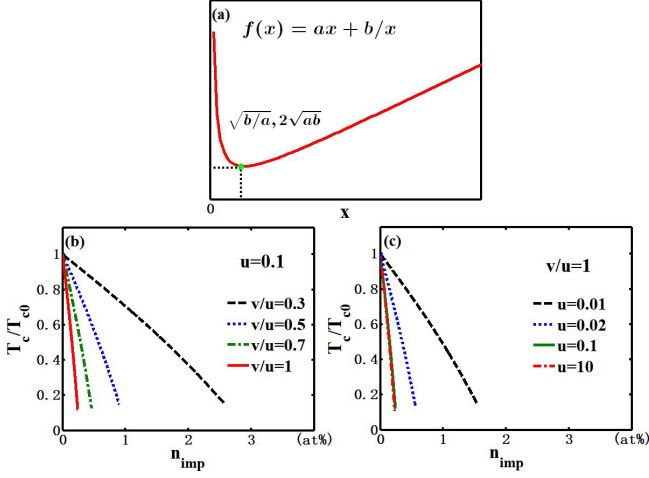


FIG. 4: (a) The Hook function of the standard form, $f(x) = ax + b/x$, with a crossing point at $(\sqrt{b/a}, 2\sqrt{ab})$. (b) T_c/T_{c0} as a function of the impurity concentration n_{imp} with varying ratio v/u at $u = 0.1$. (c) T_c/T_{c0} as a function of n_{imp} with varying intraband impurity scattering strength u at $v/u = 1$.

tonic suppression of T_c with increasing impurity concentration. On the other hand, its evolution with the impurity scattering potential is more complicated because D also depends on u and v . To see its effect more clearly, we first fix the ratio $r \equiv v/u$ and obtain $(v^2/D)^{-1} = \pi^4 N_\alpha^2 N_\beta^2 (1/r - r)^2 u^2 + 1/r^2 u^2 + \pi^2 (N_\alpha^2 + N_\beta^2)/r^2 + 2\pi^2 N_\alpha N_\beta$, which is a typical Hook function of u^2 of the standard form $f(x) = ax + b/x$ up to a constant offset. As shown in Fig. 4(a), the Hook function contains a crossing point $(\sqrt{b/a}, 2\sqrt{ab})$. We have thus a critical impurity scattering strength $U_c^2 = 1/\pi^2 N_\alpha N_\beta (1 - r^2)$ for $r < 1$ ($v < u$), which is controlled by the DOS at the Fermi energy of both bands as well as the ratio r between interband and intraband impurity scattering potentials. As a result, T_c behaves opposite across U_c . For $u < U_c$, it is more strongly suppressed as u increases, but for $u > U_c$, the superconductivity gradually revives and is robust against impurities in the unitary region. Physically, v^2/D may be regarded as the renormalized effective interband scattering, whose nonmonotonic dependence with the bare v reflects the screening of interband scattering for sufficiently large v .

To have a complete understanding of the interband impurity scattering effect, we plot in Fig. 4(b) the T_c/T_{c0} as a function of n_{imp} with varying $r = v/u$ at fixed $u = 0.1$. It is seen that T_c/T_{c0} drops very quickly with increasing r , indicating that the interband scattering plays a key role in destroying the superconductivity for the nodeless s^\pm -wave pairing. However, no anomalous behavior is seen with increasing r up to $r = 1$. This can also be understood from the Hook function by rewriting $(v^2/D)^{-1} = \pi^4 N_\alpha^2 N_\beta^2 u^2 r^2 + [\pi^4 N_\alpha^2 N_\beta^2 u^2 + \pi^2 (N_\alpha^2 + N_\beta^2) + u^{-2}]/r^2 - 2\pi^4 N_\alpha^2 N_\beta^2 u^2 + 2\pi^2 N_\alpha N_\beta$. Fixing the impurity scattering u , we obtain a critical $r_c^2 =$

$\sqrt{1 + (N_\alpha^2 + N_\beta^2)/\pi^2 u^2 N_\alpha^2 N_\beta^2 + 1/\pi^4 u^4 N_\alpha^2 N_\beta^2}$, which is always larger than unity and explains the absence of superconductivity revival in Fig. 4(b).

We note that there are two special cases: $v = 0$ and $v = u$. In the first case, we always have $v^2/D = 0$ and no suppression of T_c occurs for any value of u . This implies that pure intraband impurity scattering cannot suppress the nodeless s^\pm -wave pairing, a result in good accordance with Anderson's famous theorem³¹. The case $v = u$ has been used to study the impurity effect in iron-pnictide and other multiband superconductors^{32,33}, but not suitable for CeCu_2Si_2 . Figure 4(c) shows the results for $v/u = 1$. We see that T_c is always suppressed and drops quickly for large impurity scattering. This can be naturally understood from $(v^2/D)^{-1} = 1/v^2 + \pi^2 (N_\alpha + N_\beta)^2$ at $r = 1$, which decreases monotonically with increasing v and approaches a constant in the unitary limit.

Given the general feature of the Hook function, one may wonder if the above anomalous property should be quite generally observed in all superconductors with nodeless s^\pm -wave pairing. This is, however, not the case. In fact, as shown already in Fig. 3(d) for $\text{Ba}(\text{Fe}_{0.76}\text{Ru}_{0.24})_2\text{As}_2$, iron-pnictide superconductors also exhibit similar s^\pm -wave pairing but show more rapid T_c suppression in electron irradiation experiments than CeCu_2Si_2 (though much weaker than cuprates). To understand this, we note that the critical U_c derived above is strongly influenced by the magnitude of $(N_\alpha N_\beta)^{-1/2}$. Since the density of states N_i is inversely proportional to the quasiparticle effective bandwidth, U_c is tentatively given by the geometric average of two effective bandwidths, which is typically the order of ~ 0.1 eV in heavy-fermion systems but much higher in other multiband superconductors. For iron pnictides, first-principles calculations yield a total DOS per Fe of about 1.3 eV^{-1} per spin. The critical impurity scattering strength U_c may then be estimated to be of the order of 1 eV at $r = 0.8$, which is similar to the impurity potential 1.52 eV from Co substitution^{34,35}. Thus, while its T_c suppression may be weaker than d -wave superconductors, it is not yet fully in a region for the observation of the anomalous revival of T_c as in CeCu_2Si_2 . Our explanation is different from an earlier proposal of a possibly disorder-induced pairing transition from s^\pm to s^{++} -wave pairing³⁶. On the other hand, we speculate that this effect should be quite generally present in narrow-band systems with nodeless s^\pm -wave pairing, which might be a potential way to distinguish different pairing symmetries in, e.g., twisted bilayer graphene³⁷ or the recently discovered bilayer or trilayer Ni-based superconductors³⁸⁻⁴⁰.

To summarize, by analyzing the Eliashberg equations for a realistic two-band hybridization model and applying the T -matrix approach for its impurity effect, we reveal a critical scattering strength U_c in the presence of interband impurity scattering and nodeless s^\pm -wave pairing. When the intraband impurity scattering $u < U_c$, superconductivity is quickly suppressed as a function of the impurity concentration, while above U_c , superconductivity

revives and is found to be robust against impurities. This reconciles the controversy between doping and electron irradiation experiments, and provides important support for the fully gapped s^{\pm} -wave pairing in superconducting CeCu_2Si_2 at ambient pressure.

We acknowledge fruitful discussions with Prof. Huaiming Guo, Prof. Li Ma, and Prof. Yu Lan. This work was supported by the National Natural Science

Foundation of China (Grants No. 11774025, No. 11774401, and No. 12274036), the Strategic Priority Research Program of the Chinese Academy of Sciences (Grant No. XDB33010100), and the National Key Research and Development Program of China (Grant No. 2023YFA1406500, No. 2022YFA1402203, and No. 2021YFA1401803).

-
- * yifeng@iphy.ac.cn
† liubin@bjtu.edu.cn
- ¹ M. Smidman, O. Stockert, E. M. Nica, Y. Liu, H. Q. Yuan, Q. Si, and F. Steglich, *Rev. Mod. Phys.* **95**, 031002 (2023).
 - ² F. Steglich, J. Aarts, C. D. Bredl, W. Lieke, D. Meschede, W. Franz, and H. Schäfer, *Phys. Rev. Lett.* **43**, 1892 (1979).
 - ³ H. Q. Yuan, F. M. Grosche, M. Deppe, C. Geibel, G. Sparn, and F. Steglich, *Science* **302**, 2104 (2003).
 - ⁴ O. Stockert, E. Faulhaber, G. Zwicknagl, N. Stüßer, H. S. Jeevan, M. Deppe, R. Borth, R. KÜchler, M. Loewenhaupt, C. Geibel, and F. Steglich, *Phys. Rev. Lett.* **92**, 136401 (2004).
 - ⁵ I. Eremin, G. Zwicknagl, P. Thalmeier, and P. Fulde, *Phys. Rev. Lett.* **101**, 187001 (2008).
 - ⁶ O. Stockert, J. Arndt, E. Faulhaber, C. Geibel, H. S. Jeevan, S. Kirchner, M. Loewenhaupt, K. Schmalzl, W. Schmidt, Q. Si, and F. Steglich, *Nat. Phys.* **7**, 119 (2011).
 - ⁷ H. A. Vieyra, N. Oeschler, S. Seiro, H. S. Jeevan, C. Geibel, D. Parker, and F. Steglich, *Phys. Rev. Lett.* **106**, 207001 (2011).
 - ⁸ S. Kittaka, Y. Aoki, Y. Shimura, T. Sakakibara, S. Seiro, C. Geibel, F. Steglich, H. Ikeda, and K. Machida, *Phys. Rev. Lett.* **112**, 067002 (2014).
 - ⁹ M. Enayat, Z. Sun, A. Maldonado, H. Suderow, S. Seiro, C. Geibel, S. Wirth, F. Steglich, and P. Wahl, *Phys. Rev. B* **93**, 045123 (2016).
 - ¹⁰ S. Kittaka, Y. Aoki, Y. Shimura, T. Sakakibara, S. Seiro, C. Geibel, F. Steglich, Y. Tsutsumi, H. Ikeda, and K. Machida, *Phys. Rev. B* **94**, 054514 (2016).
 - ¹¹ G. M. Pang, M. Smidman, J. L. Zhang, L. Jiao, Z. F. Weng, E. M. Nica, Y. Chen, W. B. Jiang, Y. J. Zhang, H. S. Jeevan, P. Gegenwart, F. Steglich, Q. Si, and H. Q. Yuan, *Proc. Natl. Acad. Sci. USA* **115**, 5343 (2018).
 - ¹² T. Takenaka, Y. Mizukami, J. A. Wilcox, M. Konczykowski, S. Seiro, C. Geibel, Y. Tokiwa, Y. Kasahara, C. Putzke, Y. Matsuda, A. Carrington, and T. Shibauchi, *Phys. Rev. Lett.* **119**, 077001 (2017).
 - ¹³ T. Yamashita, T. Takenaka, Y. Tokiwa, J. A. Wilcox, Y. Mizukami, D. Terazawa, Y. Kasahara, S. Kittaka, T. Sakakibara, S. Seiro, H. S. Jeevan, C. Geibel, C. Putzke, T. Onishi, H. Ikeda, A. Carrington, T. Shibauchi, and Y. Matsuda, *Sci. Adv.* **3**, e1601667 (2017).
 - ¹⁴ Z. Wu, Y. Fang, H. Su, W. Xie, P. Li, Y. Wu, Y. Huang, D. Shen, B. Thiagarajan, J. Adell, C. Cao, H. Yuan, F. Steglich, and Y. Liu, *Phys. Rev. Lett.* **127**, 067002 (2021).
 - ¹⁵ H. Ikeda, M.-T. Suzuki, and R. Arita, *Phys. Rev. Lett.* **114**, 147003 (2015).
 - ¹⁶ Y. Li, M. Liu, Z. Fu, X. Chen, F. Yang, and Y.-F. Yang, *Phys. Rev. Lett.* **120**, 217001 (2018).
 - ¹⁷ E. M. Nica, R. Yu, and Q. Si, *npj Quantum Materials* **2**, 24 (2017).
 - ¹⁸ A. V. Balatsky, I. Vekhter, and J.-X. Zhu, *Rev. Mod. Phys.* **78**, 373 (2006).
 - ¹⁹ H. Spille, U. Rauchschwalbe, and F. Steglich, *Helv. Phys. Acta* **56**, 165 (1983).
 - ²⁰ U. Ahlheim, M. Winkelmann, C. Schank, C. Geibel, F. Steglich, and A. L. Giorgi, *Physica B* **163**, 391 (1990).
 - ²¹ A. Akbari, and P. Thalmeier, *Ann. Phys.* **428**, 168433 (2021).
 - ²² Y. Kitaoka, K. Ueda, K. Fujiwara, H. Arimoto, H. Iida, and K. Asayama, *J. Phys. Soc. Jpn.* **55**, 723 (1986).
 - ²³ K. Fujiwara, Y. Hata, K. Kobayashi, K. Miyoshi, J. Takeuchi, Y. Shimaoka, H. Kotegawa, T. C. Kobayashi, C. Geibel, and F. Steglich, *J. Phys. Soc. Jpn.* **77**, 123711 (2008).
 - ²⁴ D. D. Wang, B. Liu, M. Liu, Y.-F. Yang, and S.-P. Feng, *Front. Phys.* **14**, 013501 (2019).
 - ²⁵ S. Zhao, B. Liu, Y.-F. Yang, and S.-P. Feng, *Phys. Rev. B* **105**, 014501 (2022).
 - ²⁶ O. V. Dolgov, I. I. Mazin, D. Parker, and A. A. Golubov, *Phys. Rev. B* **79**, 060502(R) (2009).
 - ²⁷ A. V. Allen, and B. Mitrovis, *Solid State Phys.* **37**, 1 (1982).
 - ²⁸ A. V. Chubukov, D. Efremov, and I. Eremin, *Phys. Rev. B* **78**, 134512 (2008).
 - ²⁹ Y. Senga, and H. Kontani, *New J. Phys.* **11**, 035005 (2009).
 - ³⁰ M. Matsumoto, M. Koga, and H. Kusunose, *J. Phys. Soc. Jpn.* **78**, 084718 (2009).
 - ³¹ P. W. Anderson, *J. Phys. Chem. Solids* **11**, 26 (1959).
 - ³² D. Parker, O. V. Dolgov, M. M. Korshunov, A. A. Golubov, and I. I. Mazin, *Phys. Rev. B* **78**, 134524 (2008).
 - ³³ Y. Bang, H.-Y. Choi, and H. Won, *Phys. Rev. B* **79**, 054529 (2009).
 - ³⁴ A. F. Kemper, C. Cao, P. J. Hirschfeld, and H.-P. Cheng, *Phys. Rev. B* **80**, 104511(2009).
 - ³⁵ D. J. Singh and M.-H. Du, *Phys. Rev. Lett.* **100**, 237003 (2008).
 - ³⁶ D. V. Efremov, M. M. Korshunov, O. V. Dolgov, A. A. Golubov, and P. J. Hirschfeld, *Phys. Rev. B* **84**, 180512 (R) (2011).
 - ³⁷ Z. Liu, Y. Li, and Y.-F. Yang, *Chin. Phys. B* **28**, 077103 (2019).
 - ³⁸ Y.-F. Yang, G.-M. Zhang, and F.-C. Zhang, *Phys. Rev. B* **108**, L201108 (2023).
 - ³⁹ Q.-G. Yang, D. Wang, and Q.-H. Wang, *Phys. Rev. B* **108**, L140505 (2023).
 - ⁴⁰ Q.-G. Yang, K.-Y. Jiang, D. Wang, H.-Y. Lu, and Q.-H. Wang, *Phys. Rev. B* **109**, L220506 (2024).